Dissociation Energies of Sulfur-Centered Hydrogen-Bonded Complexes

DATASET · NOVEMBER 2015

3 AUTHORS, INCLUDING:

Sanat Ghosh
Tata Institute of Fundamental Research
4 PUBLICATIONS **4** CITATIONS
SEE PROFILE

Sanjay Wategaonkar
Tata Institute of Fundamental Research
72 PUBLICATIONS **948** CITATIONS
SEE PROFILE

THE JOURNAL OF PHYSICAL CHEMISTRY A

Article

pubs.acs.org/JPCA

Dissociation Energies of Sulfur-Centered Hydrogen-Bonded Complexes

Sanat Ghosh, Surjendu Bhattacharyya, and Sanjay Wategaonkar*

Department of Chemical Sciences, Tata Institute of Fundamental Research, Homi Bhabha Road, Colaba, Mumbai 400 005, India

Supporting Information

ABSTRACT: In this work we have determined dissociation energies of O−H···S hydrogen bond in the H_2S complexes of various phenol derivatives using 2-color-2-photon photofragmentation spectroscopy in combination with zero kinetic energy photoelectron (ZEKE-PE) spectroscopy. This is the first report of direct determination of dissociation energy of O−H···S hydrogen bond. The ZEKE-PE spectra of the complexes revealed a long progression in the intermolecular stretching mode with significant anharmonicity. Using the anharmonicity information and experimentally determined dissociation energy, we also validated Birge−Sponer (B-S) extrapolation method, which is an approximate method to estimate dissociation energy. Experimentally determined dissociation energies were compared with a variety of ab initio calculations. One of the important findings is that ωB97X-D functional, which is a dispersion corrected DFT functional, was able to predict the dissociation energies in both the cationic as well as the ground electronic state very well for almost every case.

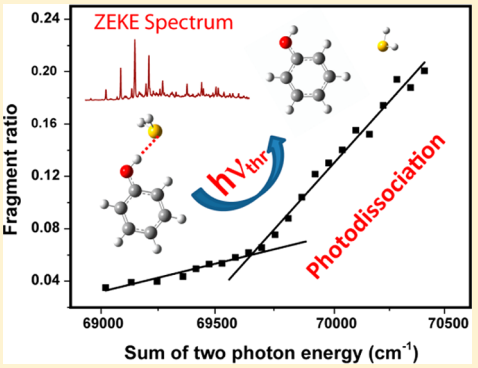

INTRODUCTION

Sulfur-centered hydrogen bonds involving RSH (R = H, alkyl groups) molecules, either as an acceptor or donor, play a vital role in determining structure of proteins and supramolecules. Structural evidence of these interactions are abundant in the crystallographic databases[1,2] and protein data bank.[3] It has also been shown that the X-H···S H-bonding interaction plays an important role in stabilizing important intermediates in enzymes such as in nitric oxide synthase (NOS).[4] Biswal et al.[5] have shown that N−H···S hydrogen bond is strong enough to influence local folding in a dipeptide structure that could be thought as one of the important factors in the folding process of proteins having S-containing residues. Recently, Mundlapati et al. have shown that N−H···S hydrogen bond is as strong as classical σ-and π-type H-bond such as N−H···O, N−H···O═C, and N−H···π H-bonds.[6]

In recent times our group has been investigating X-H···S (X = O, N) HB interactions which fall in the regime of weak or unconventional HB interaction.[7−13] Using IR-UV double resonance spectroscopy, we have shown that the X-H···S interactions exhibit all the characteristics of the conventional H-bond. However, high level computations had revealed that unlike the conventional hydrogen bonds, which are mostly stabilized by electrostatic interaction, dispersion interaction plays a vital role in stabilizing the sulfur-centered hydrogen bonds. Accounting dispersion interaction has always been challenging for the theoreticians that could lead to large errors in estimating the strength of X-H···S interactions computationally. Therefore, we took this challenge to determine the dissociation energy (depth of the potential) and intermolecular H-bond stretching frequency (shape of the potential) of the sulfur-centered H-bonded complex. If the shape and depth of potential energy surface of 1:1 interaction can be determined very precisely then this information can be utilized to build up a better force field for this class of dispersion stabilized complexes.

Earlier, we have characterized this interaction in the S_0, S_1, and recently in the cationic state.[7−15] In all of these studies, the structural characteristics of the X-H···S interaction have been investigated using IR-UV double resonance spectroscopy of the complexes in conjunction with high level of ab initio computations. Dissociation energy of the H-bonding interaction, which is a very important parameter as it controls the structure as well as functionality of hydrogen bonded complexes in large biopolymers, was estimated computationally as is done most commonly. The strength of the X-H···S H-bond has not yet been determined experimentally, although recently we reported an estimate of the dissociation energy of the O−H···S bond using the B-S extrapolation method.[15] To date, there is not a single literature report on direct determination of the X-H···S hydrogen bond energy. Even for conventional hydrogen bonds such as O−H···O or O−H···N, which have been studied extensively, there are only a few reports available that attempt to measure these interactions experimentally.[16−23]

Received: August 22, 2015
Revised: October 11, 2015
Published: October 15, 2015

DOI: 10.1021/acs.jpca.5b08185
J. Phys. Chem. A 2015, 119, 10863−10870

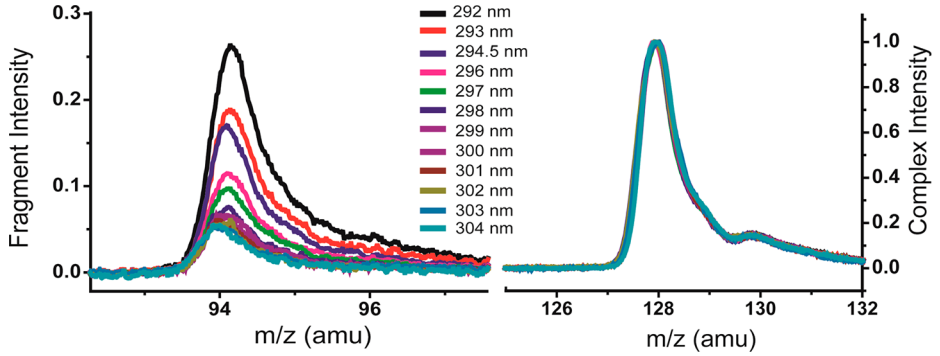

Figure 1. Mass spectra of the phenol−H_2S complex recorded at different ionization laser wavelengths; the excitation laser was set at the BO of the complex. The parent mass peak intensity at m/z = 128 amu was normalized to unity in the spectrum at each wavelength.

In this work, we report direct determination of O−H···S hydrogen bond energy for the phenol−H_2S (PH−H_2S) and *p*-cresol−H_2S (CR−H_2S) complexes using photofragmentation spectroscopy and ZEKE-PE spectroscopy. The dissociation energy in the case of *p*-chlorophenol−H_2S (CLP−H_2S) complex could not be measured directly due to the limitation of the technique, vide infra. Therefore, it was estimated by the B-S extrapolation method using the energy levels of the intermolecular stretching mode and its first few overtones observed in the ZEKE-PE spectra. We have also validated the B-S extrapolation method by comparing the dissociation energy estimated by using the B-S method with that determined using photofragmentation spectroscopy for the two complexes.

METHODS

Experimental Methods. Neusser et al. had shown for the first time that dissociation energies of noncovalently bound complexes can be obtained by determining the appearance potential of photofragments formed due to predissocation of metastable cations formed with excess energy using reflectron time-of-flight mass spectrometer.[24,25] Mons et al.[18,19,26] developed a simpler technique called photofragmentation spectroscopy based on same principles and used it to determine the dissociation energies of few systems like phenol−H_2O, phenol-MeOH, phenol-CH_3OCH_3, and few other systems in their cationic state. The technique has been discussed in detail in a review by Mons et al.[26] Briefly, it is a 2-color-2-photon technique in which the first photon excites the complex to its S_1 state band origin (BO) and the second photon ionizes it. The complex cations are detected in a time-of-flight mass spectrometer (TOFMS). When the second photon energy is in excess of the dissociation threshold of the complex cation, it predissociates into a monomer cation and a neutral solvent molecule, the efficiency of which depends on the amount of the excess energy deposited in the complex. Therefore, by scanning the second photon energy through the cation's potential well and looking for the appearance of the monomer cation in the mass spectrum gives the appearance potential (AP) of the monomer cation for the complex under investigation. The dissociation threshold of the complex both in the cationic state as well as in the ground state can be deduced by subtracting adiabatic ionization energy (AIE) of the complex and the monomer from the AP, respectively. The accurate AIEs of the monomer and the complex were obtained using ZEKE-PE spectroscopy.

A detailed description of the experimental setup has been described elsewhere.[27] Briefly, it consists of two differentially pumped stainless steel chambers (expansion chamber and ionization chamber) separated by a 2 mm skimmer. Supersonically cold molecular beam was generated by a pulsed nozzle (500 μm, General valve series 9). ZEKE-PE spectroscopy and photofragmentation experiments were performed in the ionization chamber. Pressure of the ionization chamber was kept below 1 × 10^{-6} Torr. Ionization chamber was equipped with a Wiley−McLaren type TOFMS[28] with a 20 cm flight tube (for the ZEKE-PE experiments) or a 50 cm flight tube (for the photofragment experiments). ZEKE-PE electrons were detected by the usual pulsed field ionization technique.[29,30] A Sirah Cobra Stretch-LG-18 dye laser pumped by a Nd^{3+}:YAG laser (Spectra-Physics Quanta-Ray, PRO-Series, 10 Hz, ∼10 ns fwhm) was used to excite the molecules/complexes either to the BO or to one of the vibrational states in the S_1 state and another dye laser Quantel TDL90 pumped by Brilliant-B Q-Switched Nd^{3+}:YAG laser (fwhm ∼6 ns, 10 Hz), which was temporally and spatially overlapped with the Sirah dye laser, was used to pump the excited molecules to high lying Rydberg states for the ZEKE-PE experiments or to ionize/dissociate the complexes for the photofragmentation experiments. For the ZEKE-PE experiments, the typical power of the Sirah dye laser (S_1−S_0 excitation) was kept ∼20 μJ/pulse and that for the Quantel dye laser (Rydberg−S_1) was ∼500 μJ/pulse. At the instance of interaction between the molecular beam and the UV photons, all the grids were kept grounded, and after about 1 μs the bottom and middle grids, separated by 3.2 cm, were pulsed with two fast switches (HTS50, Behlke, 20 ns rise-time) to −120 and −100 V, respectively. Temporal synchronization of the lasers and gas pulse was done by SRS Delay generator (DG645). The UV beams were copropagated through a 50 cm fl biconvex quartz lens to spatially overlap them in the molecular beam. The photofragmentation experiments were carried out in static field condition where the bottom and middle grids were kept at 3 and 2.2 kV, respectively). The excitation laser energy was kept very low ∼10 μJ/pulse and that of the ionization laser was below 100 μJ/pulse in order to avoid any one color two photon processes.

Phenol (PH), *p*-cresol (CR), and *p*-chlorophenol (CLP) were bought from Sigma-Aldrich, Zero grade H_2S (99.5%) was locally purchased from Ultra-Pure Gases (I) Pvt. Ltd. Samples were heated 70−90 °C to generate sufficient vapor pressure and the 1:1 complexes were prepared by coexpanding the sample vapor with 0.5% premix of H_2S in Helium under a stagnation pressure of 1−2 kg cm^{-2}.

Computational Methods. Ab initio calculations were performed for the H_2S complexes of the aforementioned three

DOI: 10.1021/acs.jpca.5b08185
J. Phys. Chem. A 2015, 119, 10863−10870

derivatives in their cationic state as well as their ground electronic state using Gaussian09 suit of programs.[31] Calculations were performed at the DFT level, using the B3LYP and the dispersion corrected M06-2X, ω-B97X-D functionals, and at the MP2 level. These were done on the counterpoise corrected (cp) surfaces using the augmented correlation consistent polarized valence double-ζ (aug-cc-pVDZ) basis set. The computations comprised the global minimum energy structures, vibrational frequencies, and the dissociation energies in both states. It was found that the global minimum structures for PH−H_2S, CR−H_2S, and CLP−H_2S consist of the O−H···S type of H-bond in both S_0 and D_0 state. The global minimum structures are shown in Figure S1 of the Supporting Information. The BSSE and zero point energy (ZPE) corrected dissociation energies were computed at all the levels. Additionally, the dissociation energies were also calculated at the complete basis set (CBS) limit using Helgaker's two point extrapolation method.[10,32] This extrapolation was carried out by taking the dissociation energies calculated at cp-MP2 level using the double-ζ (DZ), triple-ζ (TZ), and quadrupole zeta (QZ) basis sets. In each of the cases, the single point electronic energies were calculated on the geometry optimized at the cp-MP2/aug-cc-pVDZ method.

RESULTS AND DISCUSSION

Photofragmentation Spectroscopy of the Complexes.

In the case of phenol−H_2S complex the excitation laser frequency was fixed at its S_1 state BO (36117 cm^{-1}) and the ionization laser energy was varied. Sufficient care was taken that the ionization occurs only in the presence of both lasers. Figure 1 shows the mass spectra of phenol−H_2S complex in the region of the fragment (monomer) and the parent (complex) m/z values recorded at different ionization laser wavelengths (energies). The intensities of the mass peaks were normalized with respect to the parent (complex) mass. It is clear from the figure that the fragment ion intensity was nearly constant from 304 to 298 nm and it increased thereafter monotonically.

Figure 2 shows the fragmentation probability (fragment ratio) of the complex as a function of the sum of two photon energy. The fragment ratio at each wavelength was calculated by dividing the fragment intensity by the sum of the parent and fragment intensity. The figure shows two distinctly different regions of energy where the fragment ratio scales roughly linearly with energy, albeit with different slopes. It is very clear from the figure that beyond the dissociation threshold the fragmentation probability increases steeply. Appearance potential of phenol fragment cation was taken as 69666 ± 30 cm^{-1}, which is the sum of the two photon (S_1−S_0 BO of the complex and the ionization laser energy) energy corresponding to the intersection of the two linearly fitted plots (Figure 2). The observed AP needs field correction because the experiments were carried out under DC extraction field with field strength of 250 V/cm. The field correction (ΔE in cm^{-1}) can be calculated using the following equation[30]

$$\Delta E = 3.89\sqrt{F} \quad (\text{where, } F = \text{Field strength in Volts/cm})$$

The field corrected AP for PH−H_2S complex was 69666 + 63 = 69729 ± 30 cm^{-1} (Table 1). The fragment intensity observed below the dissociation threshold was due to some weak but unavoidable one-photon resonance followed by nonresonant two-photon ionization process in the complex leading to the fragmentation.

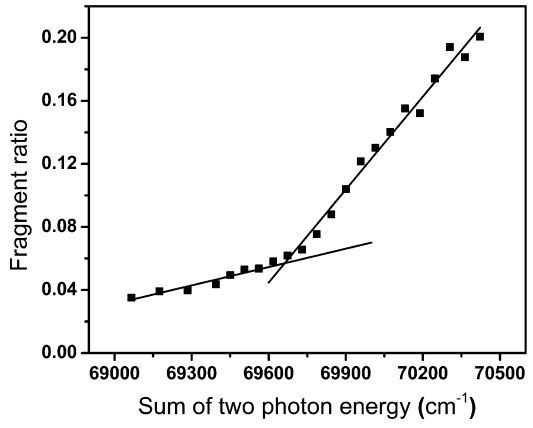

Figure 2. Plot of the fragment ratio of phenol$^+$ to the sum of the phenol$^+$ and complex$^+$ versus sum of the two-photon energy.

Table 1. Experimentally Determined Appearance Potentials (AP), Adiabatic Ionization Energies (AIE) of the Monomers and Their Complexes, and Dissociation Energies in the Ground and Cationic States[a]

species	appearance potential (AP)	adiabatic ionization energy (AIE)	cationic state dissociation energy (E_0)	ground state dissociation energy (D_0)
phenol		68628[b]		
phenol−H_2S	69729 ± 30	65543	4186 ± 30	1101 ± 30
p-cresol		65919		
p-cresol−H_2S	67077 ± 72	63133	3944 ± 72	1158 ± 72
p-chlorophenol	N/A	68099	N/A	N/A
p-chlorophenol−H_2S		65276		

[a]All values are in cm^{-1}. [b]AIE of phenol taken from ref 33.

The measurements were repeated several times on different days to obtain an average value of the appearance potential. Sufficient care was also taken to ensure that the ionization was due to a single photon process to avoid any artifacts. This was done by checking the linear dependence of the ion intensity on the ionization laser power. Because our TOF does not collect total ion flux, the relative intensities of the fragment and parent ions depend on the position of the ionization spot. Since the experiments were performed on different days, it was impossible to fix the ionization spot reproducibly. As a result, the absolute values of the fragment ratio at any given wavelength obtained on different days cannot be meaningfuly averaged. However, we can determine the dissociation threshold for each set of measurements by fitting the fragmentation probabilities as a function of the two-photon energy to two linear plots of different slopes as discussed earlier. The average value of dissociation thresholds measured in different sets of measurements can be taken as the true dissociation threshold.

Figures 1 and 2 show the data from one set of measurements out of many sets. However, the AP reported in the Table 2 is actually the average of APs determined from multiple sets of measurements. The error in AP is the one sigma standard deviation of the average value of AP. The fitting of the two straight lines was done very critically. Below the dissociation threshold several fittings were done for every set of measure-

DOI: 10.1021/acs.jpca.5b08185
J. Phys. Chem. A 2015, 119, 10863−10870

Table 2. Electronic Binding Energies, Dissociation Energies, Zero Point Corrections of the Complexes in Their Respective Ground and Cationic States Computed at Various Levels; Experimentally Determined Dissociation Energies Are Also Included[a]

	expt.	cp- ωB97X-D	cp- M06-2X	cp- B3LYP	cp- MP2	MP2/CBS (DZ-TZ)	MP2/CBS (TZ-QZ)
				[phenol−H_2S]$^+$ complex			
E_e	N/A	13.00	12.85	11.98	11.15	12.03	12.09
ΔZPE	N/A	1.21	1.13	1.12	1.38	N/A	N/A
E_0	11.97 ± 0.09	11.79	11.72	10.86	9.77	10.65	10.71
				phenol−H_2S complex			
D_e	N/A	3.92	3.90	2.82	3.82	4.23	4.28
ΔZPE	N/A	1.03	1.53	1.07	0.99	N/A	N/A
D_0	3.15 ± 0.09	2.89	2.37	1.75	2.83	3.24	3.29
ΔAIE	8.82	8.90	9.35	9.11	6.94	7.41	7.42
				[*p*-cresol−H_2S]$^+$ complex			
E_e	N/A	12.05	12.00	10.93	9.63	10.70	10.70
ΔZPE	N/A	1.26	1.80	1.02	0.93	N/A	N/A
E_0	11.28 ± 0.21	10.79	10.20	9.91	8.7	9.77	9.78
				p-cresol−H_2S complex			
D_e	N/A	3.84	3.87	2.72	3.74	4.15	4.21
ΔZPE	N/A	1.07	2.27	1.05	0.97	N/A	N/A
D_0	3.31 ± 0.21	2.77	1.60	1.67	2.77	3.17	3.23
ΔAIE	7.97	8.02	8.60	8.24	5.93	6.60	6.55
				[*p*-chlorophenol−H_2S]$^+$ complex			
E_e	N/A	12.53	12.44[b]	11.41	9.88	10.68	10.74
ΔZPE		1.06	1.21	1.03	1.36	N/A	N/A
E_0	N/A	11.47	11.23[b]	10.38	8.52	9.32	9.38
				p-chlorophenol−H_2S complex			
D_e	N/A	4.26	4.22	3.14	4.12	4.54	4.60
ΔZPE	N/A	1.21	1.60	1.12	1.03	N/A	N/A
D_0	N/A	3.05	2.62	2.02	3.09	3.51	3.57
ΔAIE	8.07	8.42	8.61	8.36	5.43	5.81	5.81

[a]All values are in kcal·mol^{-1}. [b]Cationic state optimized geometry of CLP−H_2S at M06-2X method showed a small (−5 cm^{-1}) imaginary frequency.

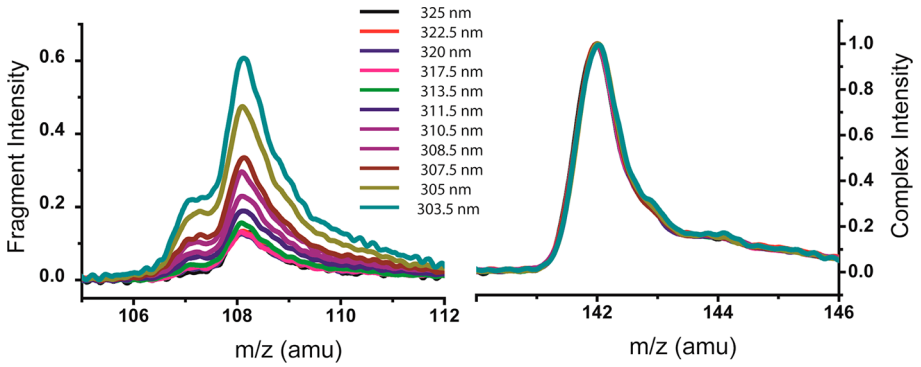

Figure 3. Mass spectra of the CR−H_2S complex recorded at different ionization laser wavelengths; the excitation laser was set at the BO of the complex. The parent mass peak intensity at m/z = 142 amu was normalized to unity in the spectrum at each wavelength.

ments as follows. For the PH−H_2S experiments, a minimum of five data points and a maximum of seven data points were taken to fit a straight line. For each of these lines, using the data points in the region above the threshold another straight line was drawn; because of the scatter near the threshold value, 2−3 data points close to the threshold were excluded. These two lines were extrapolated to intersect each other. Some fittings were done even considering the data points close to dissociation threshold. Thus, for each data set several values of dissociation threshold were obtained. The multiple values of AP from all the data sets were taken into account for averaging the AP and its standard deviation. Similarly, Figures 3 and 4 (see below) represent the results of one set of experiments of photofragmentation of CR−H_2S out of many sets performed. In this case, below dissociation threshold minimum four and maximum six data points were taken and above dissociation threshold all the data points were taken excluding 2−3 data points close to the threshold.

Figure 3 shows the mass spectra of the *p*-cresol−H_2S complex collected at different ionization laser wavelengths while exciting the complex at the S_1 state BO which was at 35098 cm^{-1}. The shoulder at 107 m/z value was due to loss of a H atom by the *p*-cresol cation. Of the three phenol derivatives investigated in this work this process was observed only for *p*-cresol. In this particular case the intensity of the 107 fragment was also accounted for while computing the fragment ratio. Figure 4 shows the fragment ratio versus the sum of two photon energy. The graph once again shows two regions of

DOI: 10.1021/acs.jpca.5b08185
J. Phys. Chem. A 2015, 119, 10863−10870

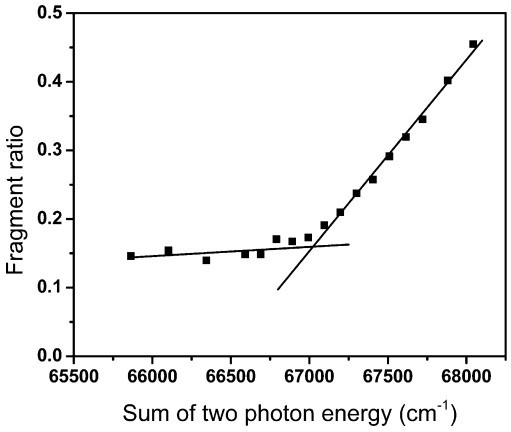

Figure 4. Plot of the ratio of p-cresol$^+$ to sum of the p-cresol$^+$ and complex$^+$ versus sum of the two-photon energy.

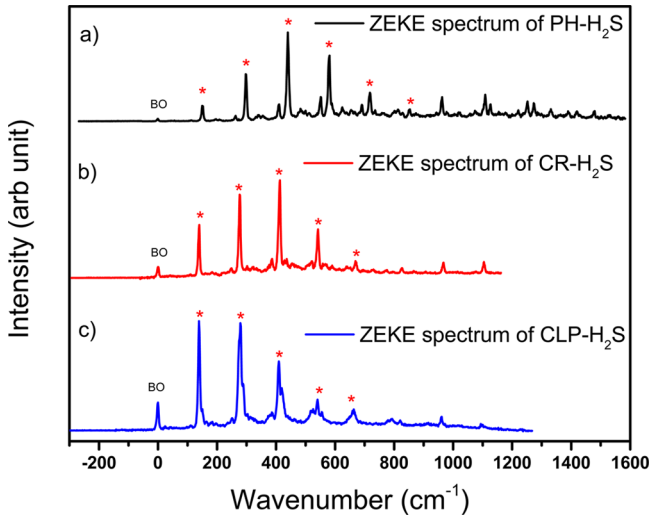

Figure 5. ZEKE-PE spectra of (a) phenol−H_2S, (b) p-cresol−H_2S, and (c) p-chlorophenol−H_2S complexes via exciting the respective S_1−S_0 BO transitions. The spectra are plotted with respect to their respective AIEs to align all the spectra in a same figure. The starred peaks indicate the progression members of the intermolecular stretch.

energy dependence. The experimental data points were fitted to two straight lines and the point of intersection was taken as the dissociation threshold for the [p-cresol−H_2S]$^+$ complex. The appearance potential (AP) for the p-cresol cation was found as 67014 ± 72 cm^{-1} in the [p-cresol−H_2S]$^+$ complex. The field corrected AP was 67014 + 63 = 67077 ± 72 cm^{-1} (Table 1).

In case of p-chlorophenol−H_2S complex the photofragmentation technique did not yield satisfactory results. The ionization laser was scanned from 33000 to 35500 cm^{-1} where the dissociation threshold was expected. Unfortunately, the plot of fragment ratio versus the laser energy (Supporting Information Figure S3) did not give two distinctly different regions. There was a lot of undesired signal due to nonresonant ionization of the monomer/complex by the ionization laser alone. The greater nonresonant ionization efficiency in this case was due to two reasons. First, the ionization laser energy was close to the BO of p-chlorophenol monomer (34809 cm^{-1}), and second the AIE of the monomer (68099 cm^{-1}) was less than the two-photon energy of the ionization laser.

ZEKE Spectroscopy of the Complexes. Figure 5 displays the ZEKE-PE spectra of the H_2S complexes of phenol, p-cresol, and p-chlorophenol, respectively, recorded via exciting their respective S_1 state band origins. For all the three complexes the BO transitions in the ZEKE-PE spectra were relatively less intense and a progression up to 5−6 quanta of the intermolecular stretch mode (σ) was observed. This suggests a significant change in geometry along this mode in the cationic state. Intermolecular stretch and its overtones are marked by stars in Figure 5. In the case of phenol complex, the progression was also observed in combination with many inter- and intramolecular vibrational transitions. These are indicated by the color-coded stars in Supporting Information Figure S6a. Complete assignments of the observed transitions are given in Supporting Information Table S3. The Franck−Condon (FC) activity among the low frequency intermolecular modes observed in the case of the phenol complex was not as apparent in the latter two cases. The origins of the ZEKE-PE spectra were observed at 65543, 63133, and 65276 cm^{-1} in the case of the phenol, p-cresol, and p-chlorophenol complexes, respectively. These were also confirmed by recording the ZEKE-PE spectra for all the three complexes via their respective σ^1 mode in S_1 state. The respective spectra are given in Supporting Information Figures S6, S7, and S8. Therefore, the AIEs were taken as 65543, 63133, and 65276 cm^{-1} for the phenol, p-cresol, and p-chlorophenol complexes, respectively.

The ZEKE-PE spectra also revealed that in all the cases the intermolecular stretch mode had significant anharmonicity, that is, the spacing between successive members of the progression decreased progressively. The details of the observed transitions and the level spacing between successive transitions are given in Supporting Information Table S4. As far as the monomers are concerned, the AIE of phenol was taken from the literature as 68628 cm^{-1}.[33] The ZEKE-PE spectra recorded for the p-cresol and p-chlorophenol monomers are shown in Supporting Information Figures S4 and S5, respectively. The AIE of p-cresol monomer was found as 65919 cm^{-1}, which is in good agreement with that reported by Tzeng et al.[34] determined by Mass Analyzed Threshold Ionization (MATI) spectroscopy. The AIE of p-chlorophenol was determined as 68099 cm^{-1}.

Dissociation Energies of the Complexes. On the basis of the appearance potentials (AP) and the AIE values of the monomers and the complexes the dissociation energies in the ground state (D_0) and in the cationic state (E_0) were obtained for the phenol−H_2S and the p-cresol−H_2S complexes. The D_0 for the PH−H_2S complex was found to be 1101 ± 30 cm^{-1} or 3.15 ± 0.09 kcal·mol^{-1}, which was about half of the D_0 (5.60 ± 0.12 kcal·mol^{-1})[19] of the PH−H_2O complex. The E_0 was found to be 4186 ± 30 cm^{-1} or 11.97 ± 0.09 kcal·mol^{-1} whereas the E_0 for the [PH−H_2O]$^+$ complex has been reported to be 18.54 ± 0.12 kcal·mol^{-1}.[19] These results indicate that the O−H···S interaction in the ground state as well as in the cationic state is weaker than the O−H···O interaction. In the similar way, the D_0 and E_0 values for the CR−H_2S complex were determined as 3.31 ± 0.21 kcal·mol^{-1} and 11.28 ± 0.21 kcal·mol^{-1}, respectively. For the p-chlorophenol−H_2S complex the dissociation energy could not be measured by the photofragmentation method.

Experimentally determined dissociation energies of these complexes are tabulated in Table 2 and are compared with the dissociation energies, calculated using different ab initio methods. Pure electronic binding energies in cationic state (E_e) and ground state (D_e) and corresponding zero point energy corrections (ΔZPE) are also included in the Table. For p-chlorophenol−H_2S complex, only the computed dissociation

DOI: 10.1021/acs.jpca.5b08185
J. Phys. Chem. A 2015, 119, 10863−10870

Table 3. Comparison of the Dissociation Energies of the Complexes in the Cationic State Determined Directly, Those Obtained Using Birge−Sponer Extrapolation Method, and cp-ωB97X-D Method[a]

dissociation energy	$[PH-H_2S]^+$	$[CR-H_2S]^+$	$[CLP-H_2S]^+$	$[FP-H_2S]^+$	$[indole-H_2O]^+$
Birge−Sponer	9.62 ± 0.68	10.86 ± 1.57	9.94 ± 1.22	9.72 ± 1.05	11.56 ± 2.30
Experimental	11.97 ± 0.09	11.28 ± 0.21			13.70 ± 0.03
cp-ωB97X-D	11.79	10.79	11.47	11.92	13.23
% deviation[b]	−20	−4	−13	−18	−16

[a]All values are in kcal·mol^{-1}. [b]Wherever the experimental value of dissociation energy was not available, the % deviation was from that computed at the cp-ωB97X-D level.

energies are given. The table also includes the dissociation energies computed at the CBS level using MP2/TZ-DZ and MP2/QZ-TZ two-point extrapolation method.[32] This method is considered as a gold standard for predicting dissociation energies of the HB complexes in ground state but it requires huge computational resources. It is apparent from the table that almost all the methods except B3LYP and M06-2X predict the ground state dissociation energies (D_0) quite well and CBS is the best among them as expected. This is quite explicable because the B3LYP functional does not account for the dispersion adequately. The M06-2X functional somehow has not been able to predict the properties of the sulfur centered H-bonded complexes that are known to be dominated by the dispersion interaction.[14] In the cationic state, however, with the exception of the ωB97X-D method all other methods failed to predict the dissociation energy (E_0) correctly, that is, almost all other methods show significant deviation. It turns out that the dissociation energies computed at the cp-ωB97X-D level were in excellent agreement with the experimental values in both the ground state as well as the cationic state. In the case of *p*-cresol−H_2S complex, the agreement is slightly less, but the change in the AIE upon complexation compares extremely well even in this case. This aspect has also been highlighted in our recent report on the ZEKE-PE spectroscopy of the FP−H_2S complex wherein the dissociation energy of the complex was estimated using the B-S extrapolation method.[15] In this regard, the cp-ωB97X-D functional turns out to be an extremely useful method that is computationally much faster compared to the CBS and the MP2 levels.

Dissociation Energies Estimated Using B-S Extrapolation. In parallel, for all the complexes the dissociation energies were estimated using B-S extrapolation method using the anharmonicity information obtained from the ZEKE-PE spectroscopic data, the details of which are explained in the Supporting Information. The dissociation energies estimated using the B-S method are compared with those determined directly and those computed at the cp-ωB97X-D/aug-cc-pVDZ level in Table 3. Data for the FP−H_2S complex, taken from our previous publication[15] was also included in the table. The estimated dissociation energies of $[PH-H_2S]^+$ and $[CR-H_2S]^+$ were compared with those determined directly using the photofragmentation method. Because the experimental energies were not available for the $[FP-H_2S]^+$ and $[CLP-H_2S]^+$ complexes, the cp-ωB97X-D method predicted numbers were taken as the true dissociation energy. It can be seen that in all the cases the B-S extrapolated dissociation energies are within 20% of the true dissociation energies on the lower side. Table 3 also includes the dissociation energy for the [indole−water]$^+$ complex reported by Braun et.al[16] determined using MATI technique as 13.70 kcal·mol^{-1}. Interestingly, the reported MATI spectrum (Figure 3 of ref 16) of the indole−water complex also shows a progression in the intermolecular stretch, albeit a very short one. They observed only the σ^1, σ^2, and σ^3 transitions, which were anharmonic in nature. We used the anharmonicity information on the intermolecular stretch and its overtones to plot the B-S extrapolation (see Supporting Information Figure S9d) and estimated the dissociation energy of that complex as 11.56 ± 2.30 kcal·mol^{-1}. The large error in the estimated value is due to fewer data points available in this case. It was found that the estimated dissociation energy from the B-S extrapolation for the [indole−water]$^+$ complex too was 16% less than the directly measured value. Calculated dissociation energy for $[indole-H_2O]^+$ using the ωB97X-D functional is 13.23 kcal·mol^{-1}, which again shows an excellent agreement with experimental dissociation energy which is 13.70 kcal·mol^{-1}.

It is very clear from the above discussion that B-S extrapolation reliably and consistently predicts the dissociation energies for this set of H-bonded complexes within 20% error limit but on the lower side. Notwithstanding the inherent approximations used in the B-S extrapolation method, it has so far been used only for diatomic molecules, that is, it has never been used for polyatomic molecules, due to the lack of clear definition of the dissociation coordinate in polyatomic molecules. We had shown[15] that as long as the intermolecular stretching mode is a pure stretching mode between the two H-bonded units, it can be safely used as the dissociation coordinate to obtain a reasonable estimate of the dissociation energy. In the present context, we validate the B-S extrapolation method as an acceptable method. The reasons for the B-S extrapolation method giving the estimates on the lower side have been discussed in ref 15.

It is apparent that the photofragmentation method is not a universal method to determine AP, that is, it has some limitations. For instance, in the event that the energy of the second photon required to predissociate the complex becomes comparable to the S_1-S_0 energy of monomer, the efficiency of the nonresonant ionization of the abundant monomers in the beam becomes appreciable, which interferes with the intensity due to those formed out of predissociation. This is precisely the situation in the case of *p*-chlorophenol. The S_1-S_0 band origin of the monomer is at 34809 cm^{-1} and the second photon energy required to predissociate the complex is predicted to be about 34695 cm^{-1} at the ωB97X-D/aug-cc-pVDZ level. Another example where the photofragmentation spectroscopy may not yield reliable values would be the cases where the predissociation lifetimes at the threshold are longer than the time scale required to escape the electric field of the grids of the TOFMS before entering the field free region.

CONCLUSION

The dissociation energies of the O−H···S H-bond were determined in this work as 3.15 ± 0.09 and 3.31 ± 0.21 kcal·mol^{-1} in the ground state and 11.97 ± 0.09 and 11.28 ± 0.21

DOI: 10.1021/acs.jpca.5b08185
J. Phys. Chem. A 2015, 119, 10863−10870

kcal·mol^{-1} in the cationic state for PH−H_2S and CR−H_2S, respectively. Compared to the O−H···O interaction these binding strengths are weaker by a factor of ∼2 in the S_0 state and ∼1.5 in the D_0 state. Surprisingly, in the case of OH···S interaction the relative increase in the H-bond strength in the cationic state with respect to that in the ground state was higher (11.97 vs 3.15 kcal·mol^{-1}) compared to the same in the case of the OH···O interaction (18.54 vs 5.6 kcal·mol^{-1}), contrary to the general expectation based on the fact that the OH···S interaction is dominated by the dispersion forces. It was also shown that the B-S extrapolation method can be safely used to estimate the dissociation energies of this class of complexes, albeit it gives within 20% lower estimation of dissociation energy. Computations using the ωB97X-D functional, which are computationally very efficient, work very well in predicting the hydrogen bond strengths across a wide variety of hydrogen-bonded complexes in the ground as well as cationic states. The dissociation energy measurement and the ZEKE spectra are the first ever complete characterization of the intermolecular H-bond stretching mode of sulfur centered H-bonded complex. We believe that our contribution will provide significant help in building up the molecular potential energy surface and predicting molecular interaction more accurately for the OH···S interactions.

■ ASSOCIATED CONTENT

Supporting Information

The Supporting Information is available free of charge on the ACS Publications website at DOI: 10.1021/acs.jpca.5b08185.

Computational results, photofragmentation data on p-chlorophenol−H_2S complex, ZEKE spectra of all the monomers as well as complexes and their detail assignment, Birge−Sponer extrapolation method and its application to estimate the dissociation energies of H-bonded complexes. (PDF)

■ AUTHOR INFORMATION

Corresponding Author

*E-mail: sanwat@tifr.res.in. Phone: +91-22-2278-2259.

Present Address

(S.B.) IAMS, Academia Sinica, P.O. Box 23-166, Taipei, Taiwan.

Notes

The authors declare no competing financial interest.

■ ACKNOWLEDGMENTS

This work was supported by the Tata Institute of Fundamental Research, Mumbai.

■ REFERENCES

(1) Viguera, A. R.; Serrano, L. Side-Chain Interactions between Sulfur-Containing Amino-Acids and Phenylalanine in Alpha-Helices. *Biochemistry* **1995**, *34*, 8771−8779.

(2) Steiner, T.; Koellner, G. Hydrogen Bonds with Pi-Acceptors in Proteins: Frequencies and Role in Stabilizing Local 3D Structures. *J. Mol. Biol.* **2001**, *305*, 535−557.

(3) Zhou, P.; Tian, F. F.; Lv, F. L.; Shang, Z. C. Geometric Characteristics of Hydrogen Bonds Involving Sulfur Atoms in Proteins. *Proteins: Struct., Funct., Bioinformatics* **2009**, *76*, 151−163.

(4) Lang, J.; Santolini, J.; Couture, M. The Conserved Trp-Cys Hydrogen Bond Dampens the "Push Effect" of the Heme Cysteinate Proximal Ligand during the First Catalytic Cycle of Nitric Oxide Synthase. *Biochemistry* **2011**, *50*, 10069−10081.

(5) Biswal, H. S.; Gloaguen, E.; Loquais, Y.; Tardivel, B.; Mons, M. Strength of NH···S Hydrogen Bonds in Methionine Residues Revealed by Gas-Phase IR/UV Spectroscopy. *J. Phys. Chem. Lett.* **2012**, *3*, 755−759.

(6) Mundlapati, V. R.; Ghosh, S.; Bhattacherjee, A.; Tiwari, P.; Biswal, H. S. Critical Assessment of the Strength of Hydrogen Bonds between the Sulfur Atom of Methionine/Cysteine and Backbone Amides in Proteins. *J. Phys. Chem. Lett.* **2015**, *6*, 1385−1389.

(7) Biswal, H. S.; Wategaonkar, S. OH···X (X = O, S) Hydrogen Bonding in Tetrahydrofurane and Tetrahydrothiophene. *J. Chem. Phys.* **2011**, *135*, 134306.

(8) Biswal, H. S.; Wategaonkar, S. O-H···O versus O-H···S Hydrogen Bonding. 3. IR-UV Double Resonance Study of Hydrogen Bonded Complexes of p-Cresol with Diethyl Ether and Its Sulfur Analog. *J. Phys. Chem. A* **2010**, *114*, 5947−5957.

(9) Biswal, H. S.; Shirhatti, P. R.; Wategaonkar, S. O-H···O versus O-H···S Hydrogen Bonding. 2. Alcohols and Thiols as Hydrogen Bond Acceptors. *J. Phys. Chem. A* **2010**, *114*, 6944−6955.

(10) Biswal, H. S.; Wategaonkar, S. Sulfur, Not Too Far Behind O, N, and C: SH···Pi Hydrogen Bond. *J. Phys. Chem. A* **2009**, *113*, 12774−12782.

(11) Biswal, H. S.; Wategaonkar, S. Nature of the N-H···S Hydrogen Bond. *J. Phys. Chem. A* **2009**, *113*, 12763−12773.

(12) Biswal, H. S.; Shirhatti, P. R.; Wategaonkar, S. O-H···O versus O-H···S Hydrogen Bonding I: Experimental and Computational Studies on the p-Cresol•H_2O and p-Cresol•H_2S Complexes. *J. Phys. Chem. A* **2009**, *113*, 5633−5643.

(13) Biswal, H. S.; Chakraborty, S.; Wategaonkar, S. Experimental Evidence of O-H-S Hydrogen Bonding in Supersonic Jet. *J. Chem. Phys.* **2008**, *129*, 184311.

(14) Bhattacharyya, S.; Bhattacherjee, A.; Shirhatti, P. R.; Wategaonkar, S. O-H···S Hydrogen Bonds Conform to the Acid-Base Formalism. *J. Phys. Chem. A* **2013**, *117*, 8238−8250.

(15) Bhattacharyya, S.; Wategaonkar, S. ZEKE Photoelectron Spectroscopy of p-Fluorophenol···H_2S/H_2O Complexes and Dissociation Energy Measurement Using the Birge-Sponer Extrapolation Method. *J. Phys. Chem. A* **2014**, *118*, 9386−9396.

(16) Braun, J. E.; Grebner, T. L.; Neusser, H. J. Van der Waals versus Hydrogen-Bonding in Complexes of Indole with Argon, Water, and Benzene by Mass-Analyzed Pulsed Field Threshold Ionization. *J. Phys. Chem. A* **1998**, *102*, 3273−3278.

(17) Burgi, T.; Droz, T.; Leutwyler, S. Accurate Hydrogen-Bonding Energies between 1-Naphthol and Water, Methanol and Ammonia. *Chem. Phys. Lett.* **1995**, *246*, 291−299.

(18) Mons, M.; Piuzzi, F.; Dimicoli, I.; Zehnacker, A.; Lahmani, F. Binding Energy of Hydrogen-Bonded Complexes of the Chiral Molecule 1-Phenylethanol, as Studied by 2C-R2PI: Comparison between Diastereoisomeric Complexes with Butan-2-ol and the Singly Hydrated Complex. *Phys. Chem. Chem. Phys.* **2000**, *2*, 5065−5070.

(19) Courty, A.; Mons, M.; Dimicoli, I.; Piuzzi, F.; Brenner, V.; Millie, P. Ionization, Energetics, and Geometry of the Phenol-S Complexes (S = H_2O, CH_3OH, and CH_3OCH_3). *J. Phys. Chem. A* **1998**, *102*, 4890−4898.

(20) Burgi, T.; Droz, T.; Leutwyler, S. Ground-State Binding-Energy and Vibrations of the Carbazole Ar Van-Der-Waals Complex by Pump Dump R2pi Measurements. *Chem. Phys. Lett.* **1994**, *225*, 351−358.

(21) Rocher-Casterline, B. E.; Ch'ng, L. C.; Mollner, A. K.; Reisler, H. Communication: Determination of the Bond Dissociation Energy (D_0) of the Water Dimer, $(H_2O)_2$, by Velocity Map Imaging. *J. Chem. Phys.* **2011**, *134*, 211101.

(22) Rocher-Casterline, B. E.; Mollner, A. K.; Ch'ng, L. C.; Reisler, H. Imaging H_2O Photofragments in the Predissociation of the HCl-H_2O Hydrogen-Bonded Dimer. *J. Phys. Chem. A* **2011**, *115*, 6903−6909.

(23) Mollner, A. K.; Casterline, B. E.; Ch'ng, L. C.; Reisler, H. Imaging the State-Specific Vibrational Predissociation of the Ammonia-Water Hydrogen-Bonded Dimer. *J. Phys. Chem. A* **2009**, *113*, 10174−10183.

DOI: 10.1021/acs.jpca.5b08185
J. Phys. Chem. A 2015, 119, 10863−10870

(24) Kiermeier, A.; Ernstberger, B.; Neusser, H. J.; Schlag, E. W. Multiphoton Mass-Spectrometry of Clusters - Dissociation Kinetics of the Benzene Cluster Ions. *J. Phys. Chem.* **1988**, *92*, 3785−3789.
(25) Ernstberger, B.; Krause, H.; Kiermeier, A.; Neusser, H. J. Multiphoton Ionization and Dissociation of Mixed Vanderwaals Clusters in a Linear Reflectron Time-of-Flight Mass-Spectrometer. *J. Chem. Phys.* **1990**, *92*, 5285−5296.
(26) Mons, M.; Dimicoli, I.; Piuzzi, F. Gas Phase Hydrogen-Bonded Complexes of Aromatic Molecules: Photoionization and Energetics. *Int. Rev. Phys. Chem.* **2002**, *21*, 101−135.
(27) Meenakshi, P. S.; Biswas, N.; Wategaonkar, S. Vibronic Spectroscopy of the H-Bonded Aminophenol-Water Complex. *J. Chem. Phys.* **2002**, *117*, 11146−11151.
(28) Wiley, W. C.; Mclaren, I. H. Time-of-Flight Mass Spectrometer with Improved Resolution. *Rev. Sci. Instrum.* **1955**, *26*, 1150−1157.
(29) Müller-Dethlefs, K.; Schlag, E. W. High-Resolution Zero Kinetic-Energy (Zeke) Photoelectron-Spectroscopy of Molecular-Systems. *Annu. Rev. Phys. Chem.* **1991**, *42*, 109−136.
(30) Lindner, R.; Dietrich, H. J.; Müller-Dethlefs, K. Basic Principles of Zeke Spectroscopy - Optimized Resolution and Accurate Ionization-Energy. *Chem. Phys. Lett.* **1994**, *228*, 417−425.
(31) Frisch, M. J.; Trucks, G. W.; Schlegel, H. B.; Scuseria, G. E.; et al. *Gaussian 09*, revision C.01; Gaussian, Inc.: Wallingford, CT, 2010.
(32) Helgaker, T.; Klopper, W.; Koch, H.; Noga, J. Basis-Set Convergence of Correlated Calculations on Water. *J. Chem. Phys.* **1997**, *106*, 9639−9646.
(33) Armentano, A.; Tong, X.; Riese, M.; Pimblott, S. M.; Müller-Dethlefs, K.; Fujii, M.; Dopfer, O. Mass Analyzed Threshold Ionization Spectra of Phenol···Ar_2: Ionization Energy and Cation Intermolecular Vibrational Frequencies. *Phys. Chem. Chem. Phys.* **2011**, *13*, 6071−6076.
(34) Lin, J. L.; Li, C. Y.; Tzeng, W. B. Mass-Analyzed Threshold Ionization Spectroscopy of p-Methylphenol and p-Ethylphenol Cations and the Alkyl Substitution Effect. *J. Chem. Phys.* **2004**, *120*, 10513−10519.

DOI: 10.1021/acs.jpca.5b08185
J. Phys. Chem. A 2015, 119, 10863−10870